Nordic Hydrology, 27 (4), 1996, 215-230

Mass Transfer Effects on Tracer Tests Conducted in a Heterogeneous Rock Fracture

Jan-Olof Selroos
Dept. of Civil and Environmental Engineering,
Royal Institute of Technology, Stockholm, Sweden

A methodology based on a combination of numerical simulation of conservative transport and an analytical solution for combined matrix diffusion and surface sorption is presented for the study of tracer tests conducted under non-uniform flow conditions in heterogeneous fractures. The methodology is based on a Monte Carlo technique with multiple realizations; hence uncertainty in transport estimates can be assessed. In an illustration example, the methodology is implemented for dipole pumping conditions (*i.e.* one injection borehole and one retrieval borehole) in a single fracture. The effect of experimental conditions such as pumping rate and tracer properties on matrix diffusion are investigated. Due to the kinetic character of the mass transfer process, it is shown that for high flow rates with consequent high advection velocities and short residence times relative to the mass transfer rate, matrix diffusion only develops to a minor extent. The effect of fracture heterogeneity is also exemplified. The results indicate that both heterogeneity in transmissivity and matrix diffusion may be manifested as tailing in solute arrival. Hence it is generally difficult to distinguish these processes under experimental conditions.

Introduction

Solute transport by groundwater in fractured rock has received much interest during the last decade due to the planned final storage of radioactive waste in the bedrock in several countries. In case of failure of the storage containers, the parent rock surrounding the waste canisters is believed to provide an adequate retention of the mi-

grating radionuclides. Chemical sorption is generally believed to be a retention process of major importance for several of the nuclides; diffusion into the rock matrix from more highly conducting fractures has also been identified as a process which may play a significant role in the retardation of nuclides (*e.g.* Neretnieks 1980). In various field tracer experiments conducted at different locations, obtained results have been interpreted in terms of an advecting solute subject to diffusion into the rock matrix (*e.g.* Abelin 1985, Frick *et al.* 1992; Novakowski and Lapcevic 1994). Analytical solutions for various cases of combined advection, dispersion and matrix diffusion in a single fracture have also been presented by several authors, *e.g.* Tang *et al.* (1981), Chen (1986), Tomasko (1987), and Cvetkovic (1991).

A general problem in the interpretation of field tracer breakthrough data is non-uniqueness, *i.e.* a number of processes can independently or in combinations adequately describe the obtained experimental results. Specifically, both heterogeneity in hydraulic parameters (*e.g.* transmissivity) and rate limited mass transfer processes (*e.g.* diffusion) yield transport results with an increased spreading and tailing of the mass; under certain circumstances these processes may be very hard to distinguish (*e.g.* Selroos and Cvetkovic 1992). For non-uniform gradients, such as flow induced by pumping, the interpretation analysis becomes even more complicated.

The objective of the present paper is to present a methodology to incorporate matrix diffusion with non-uniform transport in heterogeneous formations. Through simulation examples the combined effects of matrix diffusion and a spatially variable advection velocity on tracer tests performed in a dipole heterogeneous flow field will be analyzed in terms of expected breakthrough curves and associated uncertainties. Issues of process discrimination and prediction uncertainty will be discussed.

Mathematical Formulation and Solution Technique

Matrix Diffusion

Consider a single fracture in a rock mass under saturated conditions. The fracture lies in the x-z plane; the aperture of the fracture is $\delta(x,z)$ in the y direction. The aperture variability implies a spatial variability in transmissivity of the fracture. Depending on the specific transmissivity variability encountered and the imposed hydraulic boundary conditions, streamlines with different geometrical patterns are formed when the fracture is subject to flow. However, the length along a streamline from position $\mathbf{a}$ to position (x,z), $\lambda(x,z;\mathbf{a})$, is a single-valued function of x due to the assumption that a mean flow direction can be identified along the x axis. The velocity along a streamline is given by the function $w(\lambda)$; w is a Lagrangian-like velocity following the streamline. Different velocity functions are obtained for different streamlines. The travel time of a non-reactive (conservative) particle along a streamline from location λ_0 at the point of injection, $\mathbf{a}$, to location λ is evaluated as

$$\tau(\lambda) = \int_{\lambda_0}^{\lambda} d\lambda'/w(\lambda')$$

On each streamline the solute can diffuse in the y direction into the matrix and subsequently undergo equilibrium chemical sorption on the surfaces of the matrix. Mass-balance equations for the solute flux in the fracture, s_f(M/T), and solute flux in the matrix, s_m (M/T), may be written as

$$\begin{aligned} R_p \frac{\partial s_m}{\partial t} &\equiv D \frac{\partial^2 s_m}{\partial y^2} \\ \frac{\partial s_f}{\partial t} + w(\lambda) \frac{\partial s_f}{\partial \lambda} &\equiv k \frac{\partial s_m}{\partial y} \end{aligned} \qquad (1)$$

where the flux in the fracture is defined as the product of the local concentration, velocity and cross-sectional area of the streamline (streamtube). In Eq. (1) D is the diffusion coefficient in the matrix, $k=2D\theta/\delta_e$, where θ is the matrix porosity and δ_e is an effective aperture, $R_p=1+\rho K_d(1-\theta)/\theta$, where ρ is the density of the rock matrix (excluding pores) and K_d is a volume related, equilibrium sorption coefficient.

For an instantaneous injection along a single streamline, the solution of Eq. (1) in terms of the flux s_f normalized with the injected mass m is

$$\frac{s_f(t,\tau)}{m} = H(t-\tau) \frac{k^*\tau}{2\sqrt{\pi}(t-\tau)^{3/2}} \exp\left(\frac{-(k^*\tau)^2}{4(t-\tau)}\right) \qquad (2)$$

where $k^* \equiv k\sqrt{R_p}/\sqrt{D} = 2\theta\sqrt{DR_p}/\delta_e$, and H is the Heaviside function defined by $H(t-\tau)=1$ for $t \geq t$ and $H(t-\tau)=0$ for $t<\tau$. The solution Eq. (2) is thus expressed in terms of running time t, conservative travel time τ and the constants m and k^* only. It is noted that a simplifying assumption in Eq. (2) is that an effective (constant) mean aperture value is applicable in the calculation of k^*, even though the transmissivity of the fracture is spatially variable along the flowpath. The other assumptions implicit in the derivation of Eqs. (1) and (2) are as follows: no longitudinal dispersion, diffusion only in the y direction, well-mixed conditions over the cross-sectional area of the fracture, no advection in the matrix, and a homogeneous and infinite rock matrix. The solution in Eq. (2) is based on previous results by Tomasko (1987) and Cvetkovic (1991) for non-sorbing solutes.

The solute flux for multiple particles advecting along individual streamlines, S_f, is evaluated at coordinate x as

$$S_f(t;x) = m_{tot} \int_0^{\infty} s_f(t,\tau) p_\tau(\tau;x) d\tau \qquad (3)$$

where m_{tot} is the total solute mass along all streamlines and p_τ is a function describ-

ing the frequency of conservative arrival times at x (Selroos and Cvetkovic 1994). The function p_τ incorporates both spatial variability in transmissivity and velocity differences on the streamlines resulting from the imposed boundary conditions. It is emphasized that the length along the individual streamlines from the point of injection to location x may be different due to the boundary conditions and the meandering streamline pattern resulting from transmissivity variability.

The cumulative solute flux in the fracture, or accumulated mass M, is obtained from Eq. (3) through temporal integration as

$$M(t;x) = \int_0^t S_f(t';x)\,dt' \tag{4}$$

where S_f is defined in Eq. (3). Eqs. (3) and (4), in conjunction with the solution Eq. (2), will be used to study the effect of matrix diffusion for different pumping and heterogeneity cases in a dipole borehole configuration in a single fracture. The frequency function for conservative travel times is obtained through numerical simulation. Due to the chosen transmissivity statistics and transport conditions, the frequency function does not contain the full ensemble statistics in a single realization. Hence the solution Eq. (3) evaluated from a single realization is not the expected (ensemble mean) flux incorporating matrix diffusion, but rather one possible outcome of a matrix diffusion affected breakthrough. A Monte Carlo scheme involving multiple realizations of the travel time frequency function with subsequent multiple realizations of the matrix diffusion affected breakthroughs allows a statistical analysis where both the expected mass flux and associated uncertainty in mass flux can be estimated. However, it is noted that for conditions where the full ensemble statistics of conservative travel times are embedded in a single realization, p_τ can be interpreted as a true probability density function (pdf) of travel (residence) times. Eq. (3) is then directly the expected solute flux incorporating mass transfer (*e.g.* Cvetkovic 1991; Selroos and Cvetkovic 1992).

Numerical Simulation of Solute Advection

The numerical procedure consists of the generation of two-dimensional transmissivity fields, solving of the flow equation to obtain velocity fields, and a particle tracking scheme to obtain conservative travel times and frequency functions of particle arrival. The individual steps are briefly described below.

The spatially variable transmissivity field of the single fracture is modeled using a stochastic continuum approach. Specifically, the random fields are obtained using a methodology based on a random generator combined with a kriging technique (Rubin and Bellin 1994). The basic principle of the methodology is to first generate a random transmissivity value for one node on the grid. Second, the remaining values of the field are obtained as combinations of kriging estimates of values at neighboring nodes and random fluctuations. The generation procedure implies statistical sta-

tionarity and is based on a negative exponential covariance structure. The obtained multivariate fields follow lognormal distributions where the input statistics are given in terms of the $\log_{10}$ mean value, variance and correlation length (integral scale) of transmissivity.

The two-dimensional steady-state flow problem is defined by the equation of continuity

$$\frac{\partial}{\partial x}\left(K(x,z)\frac{\partial h}{\partial x}\right)+\frac{\partial}{\partial z}\left(K(x,z)\frac{\partial h}{\partial z}\right)=f(x,z) \tag{5}$$

where $h(x,z)$ is the hydraulic head, f is a source/sink term (T^{-1}), and K is the spatially variable hydraulic conductivity. The conductivity is obtained from the transmissivity as $K(x,z)=T(x,z)/\delta_e$, where δ_e is an effective (constant) aperture. The effective aperture is assumed to be defined through the cubic law $T_G \equiv \delta_e^3 g/12\nu$, where T_G is the geometric mean transmissivity, g is acceleration due to gravity and ν is the kinematic viscosity.

The flow solver used is based on the mixed hybrid finite element formulation (Mosé *et al.* 1994). The basic idea of the mixed hybrid formulation is to solve simultaneously for hydraulic head and velocity while satisfying an exact water balance for each element. Compared to conventional finite element formulations where the velocity is obtained through differentiation of the calculated hydraulic head, the mixed hybrid method provides velocity fields where the normal component of the velocity is continuous between adjacent elements.

As shown by Mosé *et al.* (1994), the mixed hybrid method offers particular advantages when adjacent elements in the mesh are characterized by large differences in hydraulic conductivity. Moreover, the methodology is versatile in incorporating different boundary conditions.

Transport is simulated in each flow field using a particle tracking scheme where the trajectories of inert particles are evaluated. The path of a particle along a streamline is numerically calculated as $\lambda_{t+1}=\lambda_t+w(\lambda_t)\Delta t$ where subscript t refers to a discrete point in time and Δt is the time step between two consecutive discrete points in time. The velocity $w(\lambda(x,z;\mathbf{a}))$ is calculated as a linear combination of the velocity at the four nodes of the element where the particle is located at a given point in time. Through the numerical procedure to calculate the particle pathline, the travel time at every location is automatically obtained as $\tau(\lambda_t)\equiv t$.

In each realization the matrix diffusion affected mass flux is obtained from the corresponding conservative mass flux through the integration in Eq. (3). In the solution Eq. (2) for matrix diffusion, the effective aperture is calculated using the cubic law with a transmissivity value equal to the geometric mean transmissivity. Thus the effective aperture is independent of the $\log_{10}$-transmissivity variance.

Statistics of Mass Flux

In the adopted Monte Carlo approach, equiprobable realizations of each assumed case are generated. Based on the individual breakthroughs in all realizations, the ex-

pected (ensemble mean) cumulative mass flux and variance in cumulative mass flux are estimated as

$$\bar{M}(t;x) = \frac{1}{N} \sum_{i=1}^{N} M_i(t;x) \tag{6}$$

and

$$\mathrm{var}\left(M(t;x)\right) = \frac{1}{N-1} \sum_{i=1}^{N} \left(M_i(t;x) - \bar{M}(t;x)\right)^2 \tag{7}$$

respectively. In Eqs. (6) and (7) the subscript i refers to individual realizations and N is the total number of realizations. Equations corresponding to Eqs. (6) and (7) can also be formulated for the conservative cumulative mass flux. This is done by substituting the mass flux S_f in Eq. (4) with the product $m_{tot}\rho_\tau$ and performing the integration for each realization before calculating the ensemble statistics.

Illustration Example

In the considered illustration example, the domain is discretized into 61x61 elements with each element having a dimension of 0.5x0.5 m, *i.e.* the domain is 30.5x30.5 m.

The mean of the $\log_{10}$-transmissivity is assumed to be -9.85, *i.e.* the geometric mean transmissivity is equal to 1.42×10^{-10} m^2/s. Based on this transmissivity value and the cubic law relationship, an effective aperture of 5.8 µm is obtained. The variance of the $\log_{10}$-transmissivity is in the simulation examples varied between 0.25 and 1, and the integral scale of the isotropic exponential covariance function is varied between 2 and 10 m. The integral scales thus imply four to twenty elements per integral scale. For each case considered, a total of one hundred realizations are generated.

The dipole borehole configuration is set up in the middle of the simulation domain. The injection and retrieval boreholes are both simulated as a single element in the mesh. The distance between the centers of the two boreholes is 10 m; in the direction along the two boreholes there is thus a distance of 10 m in each direction upstream and downstream of the two wells to the boundaries. In the direction perpendicular to the line connecting the two boreholes, the distance is 15 m from the wells to the boundaries. The applied boundary condition is a constant head value along all four sides of the domain. Thus there is no flow as a result of a regional gradient. The induced pumping rates are equal in both boreholes, but with opposite signs.

In the particle tracking scheme, 100 particles are released from the injection borehole and breakthrough is monitored in the retrieval borehole. In each simulation example, the time step in the particle tracking scheme is chosen so that the residence time of each inert particle in each element is sufficiently larger than the time step.

This measure is taken in order to safeguard that particles with a high velocity shall not jump adjacent elements.

Streamline Pattern

For the dipole pumping system described above, circular and symmetric streamlines between the injection and retrieval borehole result in a homogeneous system. In Fig. 1a the numerical result for eleven streamlines from a homogeneous realization is presented. The streamlines shown in the figure emanate from the injection borehole (left borehole) and all end up in the retrieval borehole (right borehole). In the injection borehole, the particles are distributed along the right boundary of the injection borehole element with equal transverse separation distances. It can be seen that the outer streamlines are longer than the inner streamlines. If successively outer streamlines had been included in the figure, *i.e.* streamlines emanating from the top and bottom boundary of the injection element, the flow field would have been wider in both the x and z directions. If particles would have been injected along the left boundary of the injection element, even a wider flow field would result. As a limiting case, the widest streamline would go in the negative direction along the line connecting the two wells.

In Fig. 1b the same flow situation as in Fig. 1a is shown for a realization with spatial variability in transmissivity. For the particular case considered, the transmissivity statistics are given by a variance $\sigma_Y^2=1$ and an integral scale I_Y =2 m, where $Y=\log_{10}(T)$. Due to the heterogeneity in transmissivity, the streamlines are distorted. From the streamline configuration it can be concluded that the upper part of the flow domain has higher transmissivity regions than the lower part. Furthermore, even

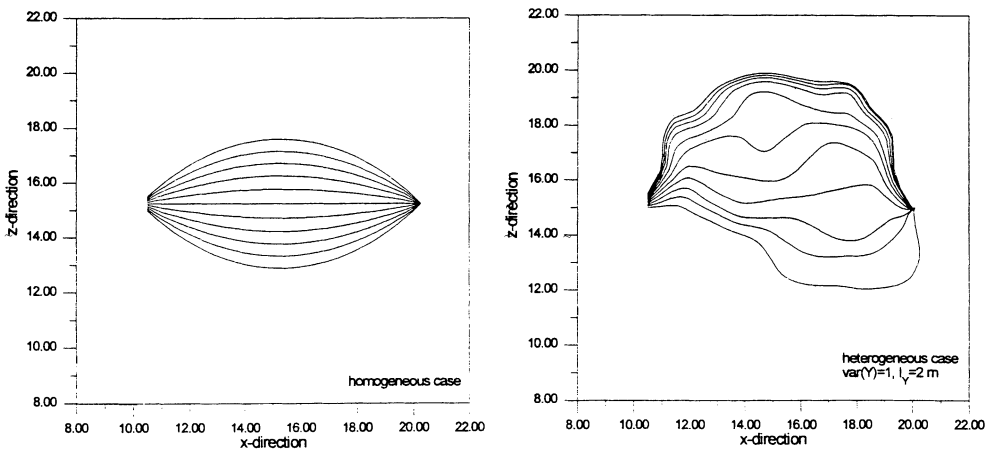

Fig. 1. Streamlines resulting from the dipole flow configuration for a) a homogeneous case, b) a heterogeneous case with a transmissivity variance $\sigma_Y^2=1$ and an integral scale I_Y =2 m.

though all streamlines of the considered realization end up in the retrieval borehole, realizations where this is not the case do also exist for the considered transmissivity statistics and particle distribution in the injection element. This is due to the fact that the high variability results in some streamlines crossing the boundaries of the domain. Given the finite size of the simulation domain, some particles are thus lost.

When numerical breakthroughs are monitored for the cases shown in Fig. 1a and 1b there will be a full mass recovery. Compared to real experimental conditions where mass is injected around the whole circumference of the injection borehole, the obtained numerical breakthroughs may be considered normalized with the fraction of mass migrating along the fastest inner pathlines (*i.e.* the pathlines included in Fig. 1). The procedure is in agreement with the fact that experimental breakthrough analyses are frequently made on the early part of mass arrival; practical time constraints limit measurements at the end of a dipole induced mass arrival tail. With increased heterogeneity, the fraction of mass lost may be increased as indicated in the discussion above related to Fig. 1b.

Effect of Mass Transfer Rate and Pumping Rate

In Fig. 2a, breakthroughs (cumulative mass fluxes) normalized with the total particle mass and corresponding to the streamlines of the homogeneous case shown in Fig. 1a are presented for a pumping case of Q=5 ml/h. Both conservative and diffusion affected breakthroughs are presented. It is observed that since only the inner and faster streamlines are included, the breakthrough in Fig. 2a is close to that of a pulse. If more outer streamlines had been included in Fig. 1a, the conservative breakthrough in Fig. 2a would have been more dispersed.

The effect of matrix diffusion is shown for three different values of the rate parameter k^*. The middle case with k^*=0.1 $h^{-1/2}$ corresponds to the assumed constant aperture δ=5.8 μm, a matrix porosity θ=0.001, a diffusion coefficient D=2.5×10^{-11} m^2/s, and a retardation factor R_p=1. The diffusion and porosity values are chosen to be representative of impermeable, dense crystalline rock. The other two cases represent a two-fold increase and decrease in the rate parameter, respectively. It is seen in Fig. 2a that the main feature of matrix diffusion is a delay in mass arrival and pronounced tailing. For diminishing values of k^* the solution converges to the nonreactive case, whereas for increasing values the cumulative mass flux approaches zero. Increasing k^*-values imply an increase in the diffusion parameter, an increase in the retardation coefficient, an increase in the matrix porosity, or a decrease in the aperture.

In Fig. 2b the effect of the pumping rate on the homogeneous conservative breakthrough and homogeneous matrix diffusion affected breakthrough with k^*=0.1 $h^{-1/2}$ is shown. The breakthroughs correspond to the streamlines presented in Fig. 1a. Increasing or decreasing the pumping rate by a factor of five shifts the conservative breakthrough by a factor of five prior or posterior in time. It is observed that for the lowest pumping rate the dipole pumping scheme has the strongest influence on the

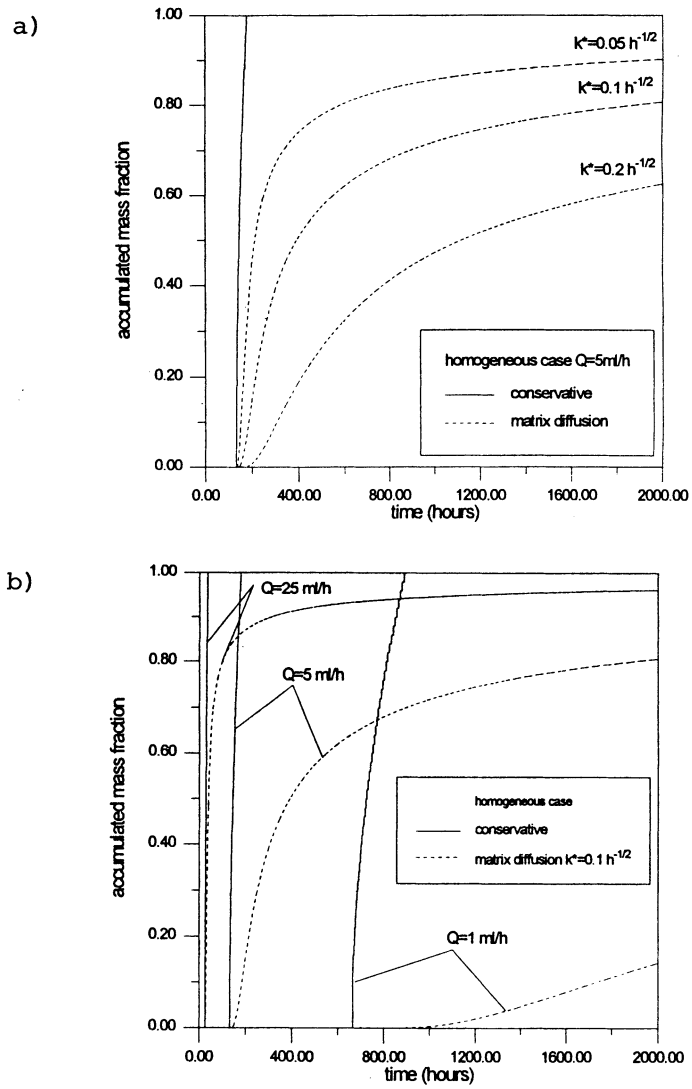

Fig. 2. Cumulative mass fluxes of a conservative solute and matrix diffusion affected solutes in the homogeneous transmissivity case. a) Effect of matrix diffusion rate parameter k^* on the cumulative mass fluxes. b) Effect of pumping rate on the cumulative mass fluxes.

conservative breakthrough in terms of tailing. However, the assumption of particle distribution in the injection element should be remembered; in a real dipole case, tailing will exist even at high pumping rates due to the fact that mass advecting on outer streamlines may be incorporated in the breakthrough.

It is also noted in Fig. 2a that the pumping rate has a markedly stronger effect on the shape of the matrix diffusion affected breakthroughs than on the conservative ones. Thus, increasing the pumping rate by a factor of five results in a matrix diffusion affected breakthrough which is very similar to the corresponding conservative breakthrough up to an accumulated mass value of approximately 0.8. Above this accumulated mass value, the breakthrough is manifested by strong tailing. Decreasing the pumping rate by a factor of five results in a matrix diffusion affected breakthrough which is strongly delayed and which shows pronounced tailing already from the first mass arrival. The difference in behavior is explained by the fact that diffusion is a kinetic (rate controlled) type of process. With higher pumping rates, thus implying higher velocities and shorter travel times compared to the characteristic time for mass transfer, matrix diffusion will not develop to the same extent and the solute will behave more as a conservative tracer.

Effect of Spatial Variability in Transmissivity

When spatial variability in transmissivity is included, multiple Monte Carlo realizations are used as described above. In Fig. 3 the breakthroughs of five conservative realizations and five corresponding matrix diffusion affected realizations with k^*=0.1 $h^{-1/2}$ are presented. The variability is defined by a variance σ_Y^2=1 and an integral scale I_Y=2 m, *i.e.* the same transmissivity statistics as in the single realization in Fig. 1b. The pumping rate is 5 ml/h.

It is observed in Fig. 3 that in one of the conservative realizations full mass recovery is not attained. The other four conservative realizations are characterized by various amounts of tailing in breakthrough. The matrix diffusion affected breakthroughs show a variability in mass recovery corresponding to the variability in the conservative breakthroughs; *i.e.* the fastest conservative breakthrough realization yields the matrix diffusion affected realization with highest mass recovery, whereas conservative realizations with delay in mass recovery yield matrix diffusion affected breakthroughs with lower mass recoveries. Furthermore, when the integration Eq. (3) is performed on the individual conservative realizations, it is observed that a smoothing effect is obtained on the matrix diffusion affected breakthroughs.

Comparing the conservative cases of Figs. 2a and 3, it is seen that in some realizations heterogeneity results in first arrival of mass earlier than in the homogeneous case, whereas in other realizations heterogeneity results in later first arrival of mass. Furthermore, some heterogeneous realizations are characterized by increased delay and tailing in mass arrival as compared to the homogeneous case, whereas other realizations have full recovery prior to the homogeneous case. Comparing the matrix diffusion affected breakthroughs, it is observed that the homogeneous case is intermediate in mass recovery relative to the heterogeneous cases. Furthermore, the matrix diffusion affected breakthrough of the homogeneous case (Fig. 2a) is very similar to the conservative realization with incomplete mass recovery of the heterogeneous case (Fig. 3). Moreover, this conservative breakthrough and the diffusion affect-

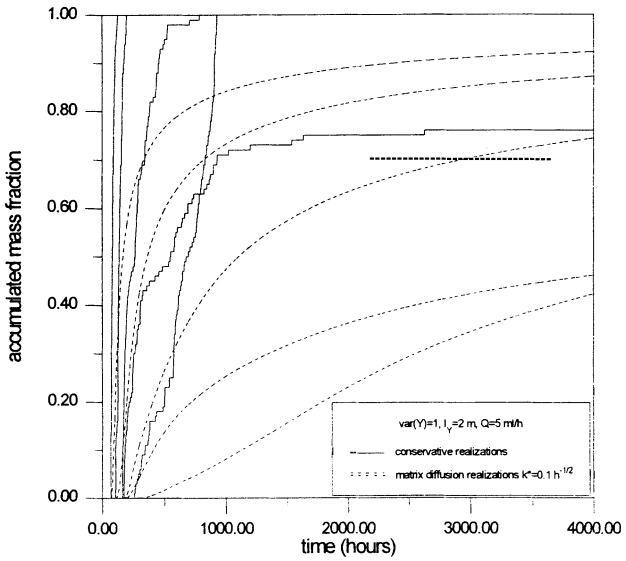

Fig. 3. Individual cumulative mass flux realizations of a conservative solute and a matrix diffusion affected solute with k^*=0.1 $h^{-1/2}$ for a heterogeneous transmissivity case with σ_Y^2=1 and I_Y =2 m.

ed breakthroughs with highest mass recovery of the heterogeneous case show similar breakthrough characteristics. Thus, given only a single experimental breakthrough, it may be impossible to discriminate between the different processes contributing to the tail.

Resulting Mass Flux Statistics

In Fig. 4 the breakthrough statistics of an ensemble of one hundred (N=100) realizations are shown as the expected (ensemble mean) cumulative mass flux and uncertainty envelopes calculated as the expected cumulative mass flux +/- one standard deviation. The envelopes are defined with a minimum value of zero and a maximum value of one. The expected value and variance are calculated according to Eqs. (6) and (7), respectively. Both conservative breakthroughs and matrix diffusion affected breakthroughs with k^*=0.1 $h^{-1/2}$ are presented.

In Fig. 4a the same transmissivity statistics as in Fig. 3, *i.e.* σ_Y^2=1 and I_Y =2 m, are used. Comparing Fig. 4a with the corresponding homogeneous case in Fig. 2a, it can be noticed that for the heterogeneous case the ensemble mean breakthrough has some mass arrival prior to the homogeneous case. Furthermore, it is observed that for the heterogeneous case the ensemble mean conservative breakthrough does not have full mass recovery. This is due to the fact that some individual realizations are characterized by incomplete mass recovery. Comparing the matrix diffusion affected breakthroughs, it is observed that the ensemble mean of the heterogeneous case has

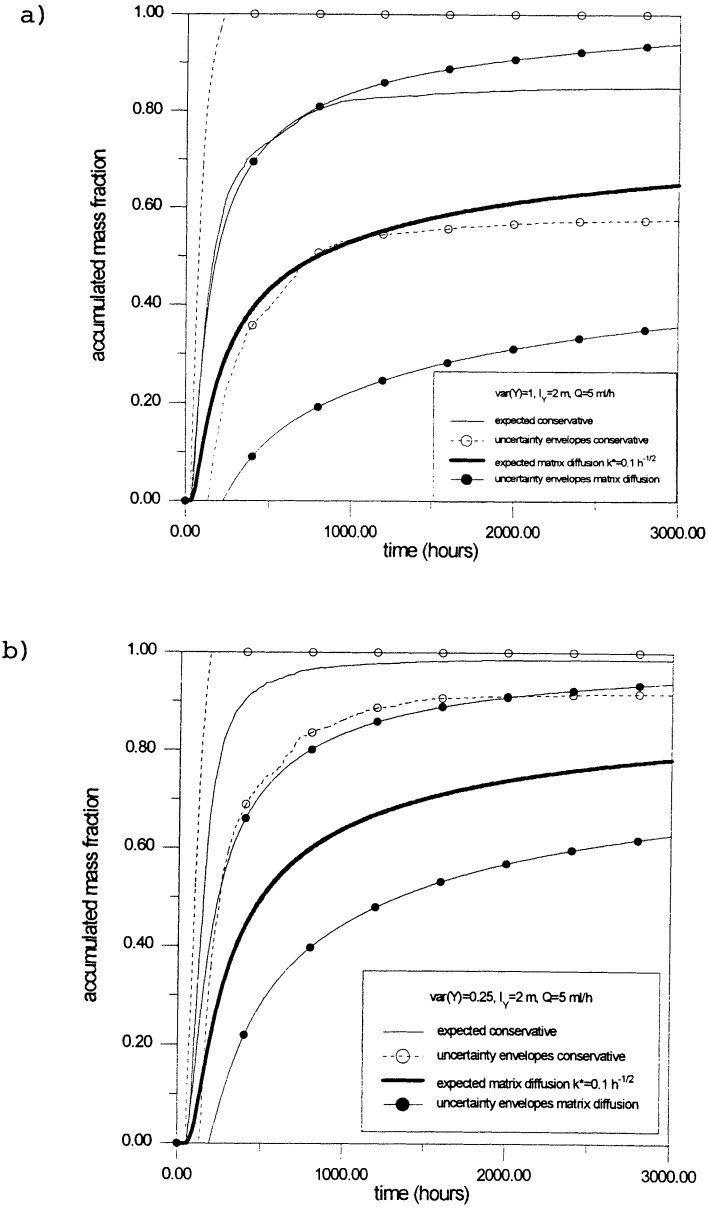

Fig. 4.

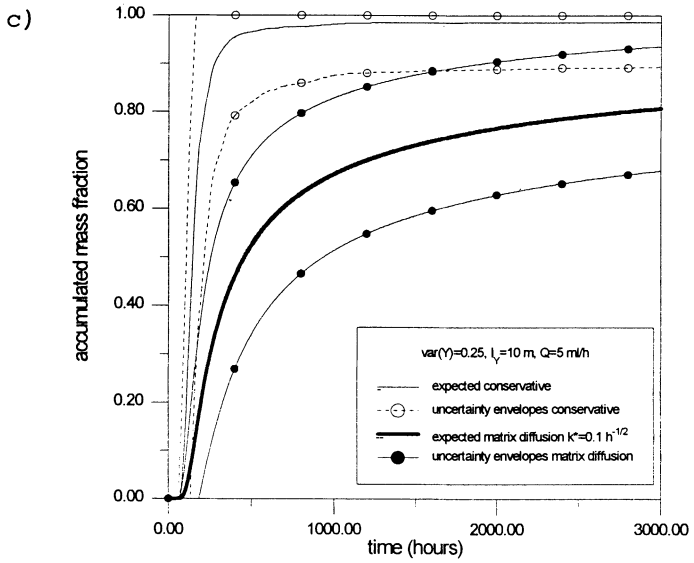

Fig. 4. Expected cumulative mass flux of a conservative solute and a matrix diffusion affected solute with k^*=0.1 h$^{-1/2}$ and corresponding uncertainty envelopes defined as the expected cumulative mass flux +/- one standard deviation for a) σ_Y^2=1 and I_Y =2 m, b) σ_Y^2 =0.25 and I_Y =2 m, and c) σ_Y^2 =0.25 and I_Y =10 m.

lower mass recovery than the homogeneous case. However, the mass recovery of the homogeneous case lies within the uncertainty envelopes of the heterogeneous case.

Comparing the uncertainty envelopes of the conservative and matrix diffusion affected breakthroughs in Fig. 4a, it is noticed that the matrix diffusion case is characterized by slightly lower uncertainty during early breakthrough and by slightly larger uncertainty during the tailing phase. This is a result of early mass recovery differences between individual realizations in the conservative case being manifested for the matrix diffusion case at later times (Fig. 3).

In Fig. 4b the variance of the transmissivity has been reduced to σ_Y^2=0.25. Compared to the case with higher variability in Fig. 4a, it is noted that both the conservative and matrix diffusion affected breakthroughs converge to the corresponding homogeneous cases of Fig. 2a. Specifically, the expected mass recovery is increased in the low variability case in Fig. 4b as compared to the case in Fig. 4a. Furthermore, the uncertainty envelopes are reduced for both the conservative and matrix diffusion affected breakthroughs when the transmissivity variance is reduced. With less spatial variability, our prediction ability thus increases.

In Fig. 4c the transmissivity statistics are given by σ_Y^2=0.25 and I_Y =10 m, *i.e.* the same case as in Fig. 4b except for a five-fold increase in correlation length. An increased integral scale (correlation length) compared to the simulation domain implies more nonergodic conditions (*e.g.* Dagan 1989). It is observed that with the in-

creased correlation length, the conservative breakthrough is characterized by a slightly higher mass recovery prior to approximately t=1000 hours. After t=1000 hours, the recoveries are identical. The explanation for this behavior is that with increased correlation lengths, and hence increased probability of two adjacent elements having transmissivity values close in magnitude, the advecting particles experience relatively more homogeneous conditions. The increased homogeneity implies higher conservative mass recoveries at early times in the individual realizations.

For the presented matrix diffusion case, the effect of an increased correlation length on the expected breakthrough is a higher mass recovery during the tailing phase; this is a consequence of the higher early mass recovery of the conservative case. Comparing the uncertainty envelopes of Fig. 4b and 4c, it is observed that the increased correlation length in Fig. 4c implies slightly smaller envelopes for the matrix diffusion affected breakthrough. For the conservative breakthrough, the uncertainty envelopes are smaller for the increased correlation length case for times prior to t=1000 hours, *i.e.* for times with a higher expected mass recovery than in Fig. 4b.

The phenomenon of increased mass recovery in the expected breakthrough complemented with smaller prediction uncertainty when increasing the correlation length is in contrast to unidirectional flow with a constant gradient where mass arrival is monitored over a cross section perpendicular to the mean flow direction. For the latter flow configuration an increased correlation length results in an expected cumulative mass flux with larger temporal spread and hence lower expected mass recovery at the point in time characterized by nearly full recovery in a case with shorter correlation length (*e.g.* Selroos and Cvetkovic 1992, Cvetkovic *et al.* 1992). Specifically in a single fracture context, the same feature has been shown in terms of increased dispersion for increasing correlation lengths (Ewing and Jaynes 1995). Furthermore, for the point in time characterized by nearly full recovery in the unidirectional case with shorter correlation length, the uncertainty envelopes will be smaller than for a case with longer correlation length and more incomplete recovery (Cvetkovic *et al.* 1992). Thus, the simulation example of the present study indicates that transport under nonergodic conditions in a dipole flow configuration with possible incomplete mass recovery may be manifested by breakthrough moments showing different behavior than the corresponding moments for a constant gradient flow case.

For the cases with variability in transmissivity, the mass transfer and pumping rates have not been varied in the presented simulation examples. However, the general features of a change in these parameters are the same as for the homogeneous case. This is due to the fact that a changed pumping rate only shifts the conservative breakthrough, and to the fact that the matrix diffusion is characterized by an effective rate parameter independent of the transmissivity variability. However, the effective rate parameter k^* could be based on the arithmetic or harmonic mean values of transmissivity, rather than the geometric mean value, and hence implicitly incorpo-

rate a dependence on the transmissivity variance σ_Y^2. With the variances considered in the simulation examples presented in this study, the changes in the rate parameter k^* corresponding to the harmonic or arithmetic mean transmissivity values would be minor.

Summary and Conclusions

A simple method for incorporating combined surface sorption and matrix diffusion under non-uniform flow conditions in a heterogeneous fracture has been presented. Conservative breakthroughs obtained through any numerical simulation scheme can serve as input for the matrix diffusion affected breakthroughs. The method is fast and efficient due to the analytical character of the incorporated mass transfer solution. With a Monte Carlo approach consisting of multiple realizations, the prediction uncertainty can be assessed.

The method is exemplified for a single fracture. The results indicate that both heterogeneity and matrix diffusion may be manifested by delay and tailing in mass arrival. Furthermore, the imposed dipole boundary conditions also imply spreading in breakthrough. Hence it may be difficult to distinguish these processes under field conditions. However, the simulation method presented in this work may be used in the design of tracer experiments such that subsequent analysis and process discrimination of breakthrough data is simplified. Specifically, through numerical simulations the order of magnitude of k^* in conjunction with utilized pumping rates can be optimized in order to yield or inhibit matrix diffusion.

The dependence of the mass flux on transmissivity variance and correlation length is also shown in the illustration examples. Increasing transmissivity variability implies an increased prediction uncertainty. A decreasing experimental scale relative to the heterogeneity scale results in more homogeneous mass flux characteristics, *i.e.* earlier expected breakthroughs complemented with decreased prediction uncertainty.

The obtained methodology is believed to be of interest in the analysis of tracer experiments conducted in order to investigate the possible importance of matrix diffusion as a viable retardation process for radionuclides migrating in fractured rock (Selroos *et al.* 1994).

Acknowledgements

The author wishes to thank Vladimir Cvetkovic, Department of Civil and Environmental Engineering, Royal Institute of Technology, Stockholm for discussions on the work and comments on the manuscript. Financial support by the Swedish Nuclear Fuel and Waste Management Co (SKB) is acknowledged.

References

Abelin, H., Neretnieks, I., Tunbrant, S., and Moreno, L. (1985) Final report of the migration in a single fracture – experimental results and evaluation. International OECD/NEA Stripa Project, SKB Stripa Technical Report TR 85-03, Stockholm, Sweden.

Chen, C. H. (1986) Solutions for radionuclide transport from an injection well into a single fracture in a porous formation, *Water Resour. Res., Vol. 22*, pp. 508-518.

Cvetkovic, V. (1991) Mass arrival of reactive solute in single fractures, *Water Resour. Res., Vol. 27*, pp. 177-183.

Cvetkovic, V., Shapiro A. M., and Dagan, G. (1992) A solute flux approach to transport in heterogeneous formations, 2. Uncertainty analysis, *Water Resour. Res., Vol. 28*, pp. 1377-1388.

Dagan, G. (1989) *Flow and transport in porous formations*, Springer Verlag.

Ewing, R. P., and Jaynes, D. B. (1995) Issues in single-fracture transport modeling: Scales, algorithms, and grid types, *Water Resour. Res., Vol. 31*, pp. 303-312.

Frick, U. *et al.* (1992) The radionuclide migration experiment – overview of investigations 1985-1990. NAGRA Technical Report 91-04, Wettingen, Switzerland.

Mosé, R., Siegel, P., and Ackerer, P. (1994) Application of the mixed hybrid finite element approximation in a groundwater flow model: Luxury or necessity? *Water Resour. Res., Vol. 30*, pp. 3001-3012.

Neretnieks, I. (1980) Diffusion in the Rock Matrix: An Important Factor in Radionuclide Retardation? *J. Geophys. Res., Vol. 85*, pp. 4379-4397.

Novakowski, K. S., and Lapcevic, P. A. (1994) Field measurement of radial solute transport in fractured rock, *Water Resour. Res., Vol. 30*, pp. 37-44.

Rubin, Y., and Bellin, A. (1994) Hydrogen: A new random field generator for correlated properties, Geotechnical Engineering Report No. UCB/GT/94-04, University of California at Berkeley.

Selroos, J. O., and Cvetkovic, V. (1992) Modeling solute advection coupled with sorption kinetics in heterogeneous formations, *Water Resour. Res. Vol. 28*, pp. 1271-1278.

Selroos, J. O., and Cvetkovic, V. (1994) Mass flux statistics of kinetically sorbing solute in heterogeneous aquifers: Analytical solution and comparison with simulations, *Water Resour. Res., Vol. 30*, pp. 63-69.

Selroos, J. O., Winberg, A., and Cvetkovic V. (1994) Design constraints and process discrimination for the detailed scale tracer experiments at Äspö. Multiple well tracer experiment and matrix diffusion experiment, Swedish Nuclear Fuel and Waste Management Co, SKB ICR 94-04.

Tang, D. H., Frind, E. O., and Sudicky E. A. (1981) Contaminant transport in fractured porous media: Analytical solution for a single fracture, *Water Resour. Res., Vol. 17*, pp. 555-564.

Tomasko, D. (1987) The Effects of a Bimodal Pore Distribution on Matrix Diffusion in a Fractured Porous Medium, Sandia report SAND87-0265, UC-70.

First received: 15 August, 1994
Revised version received: 12 October, 1995
Accepted: 30 November, 1995

Address:
Dept. of Civil and Environmental Eng.,
Royal Institute of Technology,
S-100 44 Stockholm,
Sweden.